COMPARISON OF SEISMIC PERFORMANCE OF BASE-ISOLATED HOUSE WITH VARIOUS DEVICES

Tsutomu HANAI[1], Shinji NAKATA[2], Shin-ichi KIRIYAMA[3], and Nobuo FUKUWA[4]

SUMMARY

Recently, various base-isolated devices corresponding to the low-rised house have been developed in practical use. However, the common information for designers to select specific device has not been gathered. Therefore, a full scale vibration test was conducted to grasp the difference of the isolated response by replacing only base-isolated devices system using common superstructure. The result of the test shows that each devices system fulfills the basic performance demanded for base-isolated houses. Each devices system is evaluated from the view points of response to each input wave, influence of vertical motion and residual displacement.

INTRODUCTION

Various base isolation devices corresponding to the low-rised house have been developed and put into practical use since the Hyogoken Nanbu Earthquake of 1995, and ball-bearing type and slide type base isolation devices have become widely used for wooden and steel-framed structures. Iiba et al.[1] conducted shaking table tests of a number of base isolation devices on development stage supporting weights. Response behavior of full-scale buildings, however, equipped with different base isolation devices (including devices and systems; the same applies hereafter) that have been put into practical use thus far have not yet been compared and verified under the same conditions. At present, designers are not given information that would enable them to select appropriate base isolation devices according to such factors as the characteristics of input ground motions, building site restrictions, and the owner's preferences.

The authors therefore conducted a vibration test using a shaking table capable of simultaneous three-axis excitation. In the test, different base isolation devices were tested with the same superstructure placed on the shaking table in order to compare the responses obtained with the different base isolation devices. The

---

[1] Nihon System Sekkei Co.,Japan.Email:hanai@nittem.co.jp
[2] Asahi Kasei Homes Co.,M.Eng.,Japan.Email:nakata.sb@om.asahi-kasei.co.jp
[3] Asahi Kasei Homes Co.,M.Eng.,Japan.Email:kiriyama.sb@om.asahi-kasei.co.jp
[4] Prof., Dept. of Environmental Engineering and Architecture, Graduate School of Environmental Studies, Nagoya Univ., Dr.Eng.,Japan.Email:fukuwa@sharaku.nuac.Nagoya-u.ac.jp

base isolation devices used in the test were two types of ball-bearing devices (A, B) and one type of sliding devices (C).

In the test, ground motions of near-field inland earthquakes and of ocean trench earthquakes containing long period components were used as input ground motions. Medium-level to close-to-2G horizontal excitation and simultaneous three-axis excitation involving more-than-1G vertical motions were conducted to investigate response changes due to different levels of input and the effects of vertical motion inputs on response. The test building was provided with finishing and with high-aspect-ratio furniture to observe damage due to superstructure response. The test results were examined to identify the characteristics of the responses obtained with different types of base isolation devices. And information useful for the performance-based design of base-isolated houses was extracted.

FULL SCALE VIBRATION TEST

Test building
The test building consisting of a base isolation layer and a two-story superstructure was placed on a heavy-steel-frame foundation secured on a shaking table. Photo 1 and Figure 1 show the test setup, and Figure 2 shows the test building in plan view. The superstructure is a bearing panel type, post-and-beam structure built with light steel. The plan dimensions of the first floor are 6.710 m by 6.405 m; the height of the first and second stories is 2.87 m; and the total weight of the house structure including the first-floor beams is about 302 kN.
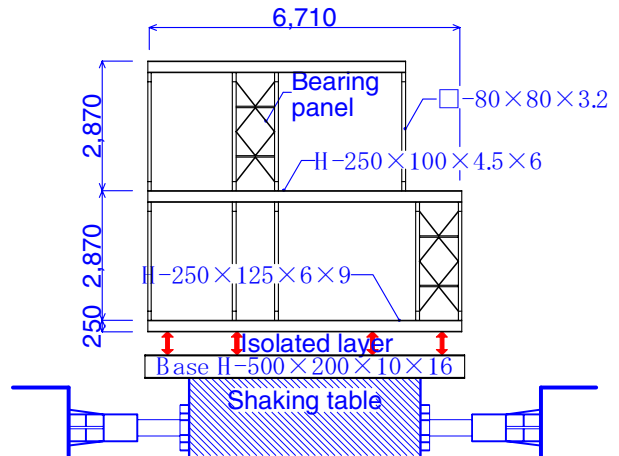

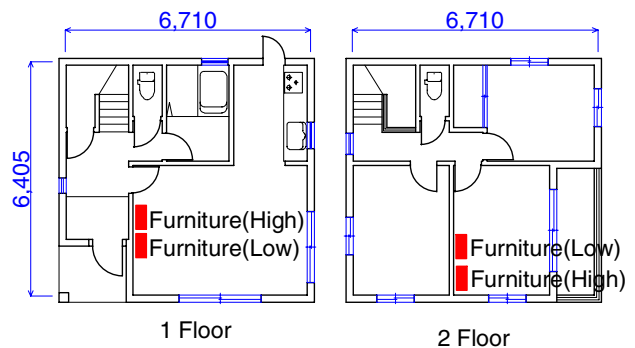**Photo 1. Test setup**

Fig.1. Test section

1 Floor   2 Floor

Fig.2. Test plan

Base isolation layer structure
The three types of base isolation devices shown in Table 1 were used in the test. Type "A" device (system; the same applies hereafter) consists of ball-type plane linear bearings, laminated rubber bearings used as a source of restoring force, and viscous dampers. The laminated rubber bearings and dampers are located so that their contribution is evenly distributed. Type B device consists of ball-in-cone bearings located along the periphery of the layer, and plane ball bearings with anti-torsion guides and viscous dampers located at the center of the layer. Restoring force is provided by the loose slope of the cone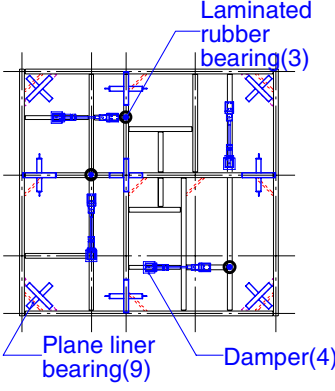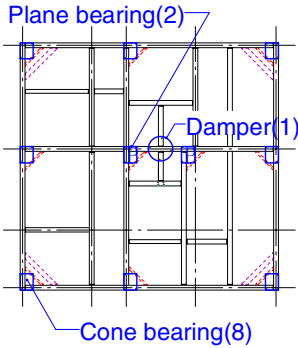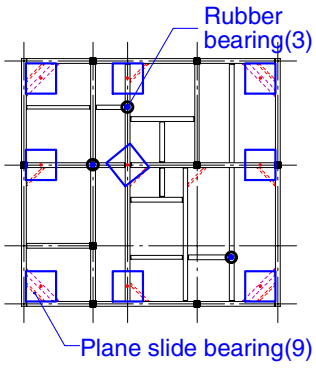, and one characteristic of this mechanism is that there is no particular period of vibration. Type C device consists of plane slide bearings combined with non-laminated rubber bearings used as a source of restoring force. The non-laminated rubber bearings are located so that their contribution is evenly distributed. This damperless device is designed to consume energy by friction. Table 1 shows the factory-set characteristic values of each device. As shown, the coefficient of frictions μ of the ball bearings and the slide bearings differ by a factor of 10 or so.

Table 1. Base isolation devices in the Test

| TYPE	Type A	Type B	Type C
Bearing	Plane linear bearing μ =0.0033 Limit $\delta=\pm400$mm	Cone bearing Plane bearing μ =0.006 Limit $\delta=\pm285$mm	Plane slide bearing μ =0.046 Limit $\delta=\pm350$mm
Restoring force	Laminated rubber bearing K=38.5N/mm Limit $\delta=\pm400$mm	Slope	Rubber bearing K=31.2N/mm Limit $\delta=\pm400$mm
Damping	Viscous damper Damping force 17kN Limit velocity 75cm/s Limit $\delta=\pm500$mm	Viscous damper Damping force 12kN Limit velocity 75cm/s Limit $\delta=\pm285$mm	—
Location	Laminated rubber bearing(3) Plane liner bearing(9) Damper(4)	Plane bearing(2) Damper(1) Cone bearing(8)	Rubber bearing(3) Plane slide bearing(9)

Excitation and measurement methods

Excitation was performed using the three-dimensional shaking table at the Technical Research Institute of Obayashi Corporation. Table 2 shows the specifications of the shaking table including the horizontal and vertical excitation capability of the shaking table.

Table 2. Specifications of the shaking table

	Horizontal	Vertical	Note
Acceleration maximum	3000cm/s^2	1000cm/s^2	Loading mass 50t
Velocity maximum	200cm/s	100cm/s	Table size 5m×5m
Displacement maximum	±60cm	±20cm	Shaking frequency DC～50Hz

Figure 3 shows the locations of the measuring instruments used. Relative displacement between the base isolation layer and the superstructure in the two horizontal directions was measured with a laser displacement meter (resolution: 0.01–0.05 mm, sampling time: 1/1,000 s). Building response was measured with strain-gauge accelerometers (effective range: 0.001G–5G). Building response in the two horizontal directions was measured at the steel frame base, first floor, second floor and roof floor levels. Building response in the vertical direction was measured at the steel frame base, first floor and roof floor levels. The acceleration of the top of each piece of furniture placed on the first and second floors was also measured in one horizontal direction and in the vertical direction. The sampling frequency used for the measurement was 200 Hz.
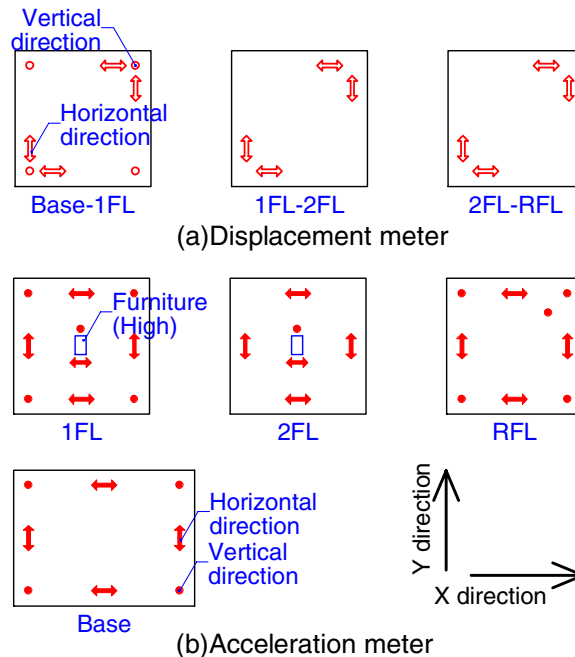
Fig.3. Measuring instrument location

Input ground motions

As shown in Table 3, the following ground motions were used as inputs: ground motions of five historical earthquakes; simulated ground motions for three types of surface ground layer with different vibration periods, T_g, of elastic ground defined in accordance with the Ministry of Construction Notification No. 1457 for the response spectra of exposed engineering bedrock described in Article 82-6 of the Building Standard Law Enforcement Ordinance ("Notification waves $_yS_a$"); and medium intensity ground motions and harmonic sine waves used for confirming the initial motion.

Figure 4 shows pseudo spectra of the Kobe, El Centro, Tarzana and Notification waves used as strong motion waves and of the medium intensity ground motion wave. The figure also shows response spectra at the steel frame base, but since a low cut filter was applied in order to protect the shaking table, the long-period components, particularly of the Notification waves, were lower than the target levels.

Excitation for the noncommented input waves was carried out to achieve the target level of 100% (the values shown in the table).

Table 3. The list of input ground motions

Input ground motions	A_{max} (cm/s^2)	V_{max} (cm/s)	D_{max} (cm)	note
El Centro 1940 NS	486	50.0	13.7	Input level:50, 100%
Taft 1952 EW	529	50.0	22.7	
Hachinohe 1968 EW	266	50.0	14.7	
Kobe(JMA) 1995 NS	813	93.3	19.0	NS wave input X directions Input level:50～150%
〃 EW	619	81.3	15.7	
〃 UD	333	41.5	13.0	
Tarzana [1] NS	971	74.5	26.5	EW wave input X directions Input level:50～100%
〃 EW	1745	114.7	26.3	
〃 UD	1028	70.5	13.4	
Notification wave1 ($_yS_a$ 050)	490	65.6	28.6	$T_g = 0.50$ s
Notification wave 2 ($_yS_a$ 075)	433	68.4	31.6	$T_g = 0.75$ s
Notification wave 3 ($_yS_a$ 100)	364	68.8	35.8	$T_g = 1.00$ s
Taft phase				Input level:50～140%
Medium intensity ground motions [2]	62~53	1.9~4.2	1.0~1.1	Shizuoka Prefecture 2001.4.3
Harmonic sine wave	Period 3s、Amplitude±10～±250mm			

*1 Northridge 1994
*2 Kyoshin Net (K-NET)

Target wave,   Measured wave
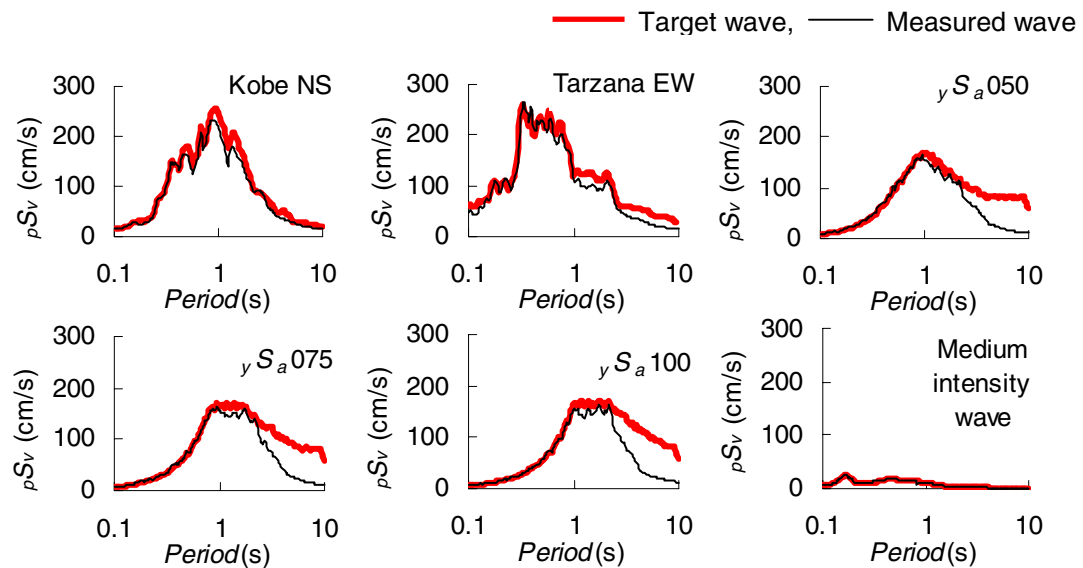
Fig.4. Pseudo spectra of the input target waves
and the measured waves at the steel frame base

Characteristics of base isolation layer and superstructure

Figure 5 shows the restoring force characteristics of the base isolation layer achieved with different types of base isolation devices. Figure 5(a) also shows the load–deformation relationship in the case where sine wave excitation of the shaking table was continued for 20 seconds (hereafter referred to as "static excitation"), along with a nominal design value model (or test values for a device alone). Figure 5(b) shows the load–deformation characteristics in the case where the superstructure was unfixed and dynamic excitation (3-second harmonic sine wave excitation) was applied to the base isolation layer. The load in this case was calculated as sum of (mass of each floor × acceleration of each floor).

In the case of a Type A device, the nominal value is calculated by adding the Y-axis intercept loads (movement initiation loads) for the ball bearings, laminated rubber bearings, and dampers. In static excitation, the load began to become larger than the nominal restoring force immediately after the initiation of rolling movement, and became about twice as large as the nominal value in the vicinity of the origin. One characteristic is that possibly because of the drum rotation mechanism, the dampers were made to carry a considerable amount of load from the stage at which the velocity was still as low as 1 to 2 cm/s (amplitude: 5 to 10 mm). In dynamic excitation, the contribution of the dampers became even greater because of velocity dependence, and the hysteresis loops were spindle-shaped.

In the case of a Type B device, which includes the ball-in-cone bearings, the slope of the inner surface of the "cone" is constant and there is no natural period of vibration. Consequently, restoring force characteristics of this device are such that the resistance load varies only in the vicinity of the origin. The amount of load carried by the ball-type bearings is very small, and in the static loading, the amount of load carried by the dampers was not very large. In the dynamic loading, however, the amount of load carried by the dampers was large, and the restoring force characteristics observed can be described as viscous. The reason why little load was carried by the dampers in the vicinity of the origin where velocity was high is thought to be that the design of the device is such that the damper head is pressed against the upper surface. Small-scale load fluctuations are due to local defects of the lower surface coating.

(a) Static excitation

(b) Dynamic excitation (3-second harmonic sine wave excitation)
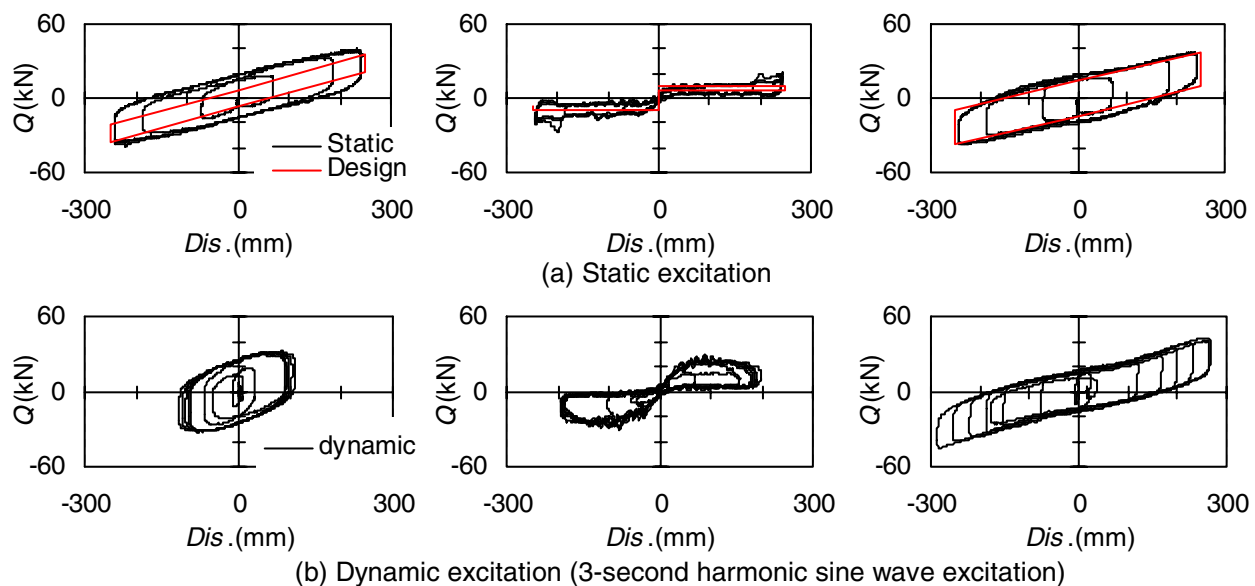
Fig.5. Restoring force characteristics of base isolation layer

In the case of a Type C device, the restoring force characteristics of the slide bearings and the nominal restoring force characteristics of the rubber bearings show close agreement in the static loading because there is no damper. More or less similar behavior was observed during the dynamic loading, indicating that velocity dependence is small.

The equivalent periods corresponding to a nominal displacement of 20 cm are 2.84 s for a Type A device, 3.71 s for a Type B device, and 2.73 s for a Type C device. The eccentricity ratio of the base isolation layer is 0.01 for a Type A device, 0.03 for a Type B device, and 0.03 for a Type C device. During the three-second harmonic sine wave excitation in which considerable displacement occurred, little torsion was observed regardless of the type of device used. As the characteristic of superstructure, the transfer functions between first floor and roof floor with the Kobe wave input shows the natural frequencies of superstructure is about 3Hz in the X and Y directions.

TEST RESULTS

Input level and maximum response value

In Figure 6, the horizontal axis shows the maximum value of the input velocity found by integrating the acceleration measured at the level of the steel frame base (immediately under the base isolation device), and the vertical axis shows the maximum values of the response displacement of the base isolation layer, the response shear coefficient at the level of each floor, and the response floor seismic intensity(JMA). "Floor seismic intensity" refers to a measured seismic intensity calculated by using the acceleration response waveform for each floor. Regardless of the type of device, the response displacement of the base isolation layer was not greater than 250 mm, the response shear modulus for the first floor and the second floor was 0.22 or less and 0.26 or less, respectively, and the floor seismic intensity was not greater than "5 upper" on the Japan Meteorological Agency's seismic intensity scale. These results confirm the effectiveness of the base isolation devices.

In the case of a Type A device, the damping mechanism began to work when the velocity was still low, so the device was effective even against medium-level ground motions with an input velocity of 10 cm/s or less. The input velocity and the shear modulus show correlation. It can be said that characteristics of linearly behaving laminated rubber bearings and viscous damping are shown. In the cases of the other devices, there was a certain degree of response to medium-level ground motions, but the amount of response was relatively small even against strong ground motions. This indicates that climbing the slope of the ball-in-cone bearing (Type B device) and exceeding the sliding friction force require a certain amount of input.

Base isolation layer displacement tended to be minimized in the case where a Type A device was used and to be maximized in the case where a Type B device, which does not depend on displacement for restoring force, was used.

Let us now take a look at responses in the cases where input acceleration level is much greater than 1G. Figure 7 shows the maximum response acceleration and the maximum response displacement in the X direction in the cases where excitation was performed by varying the input level of the Tarzana wave along two horizontal axes between 50% and 100%.
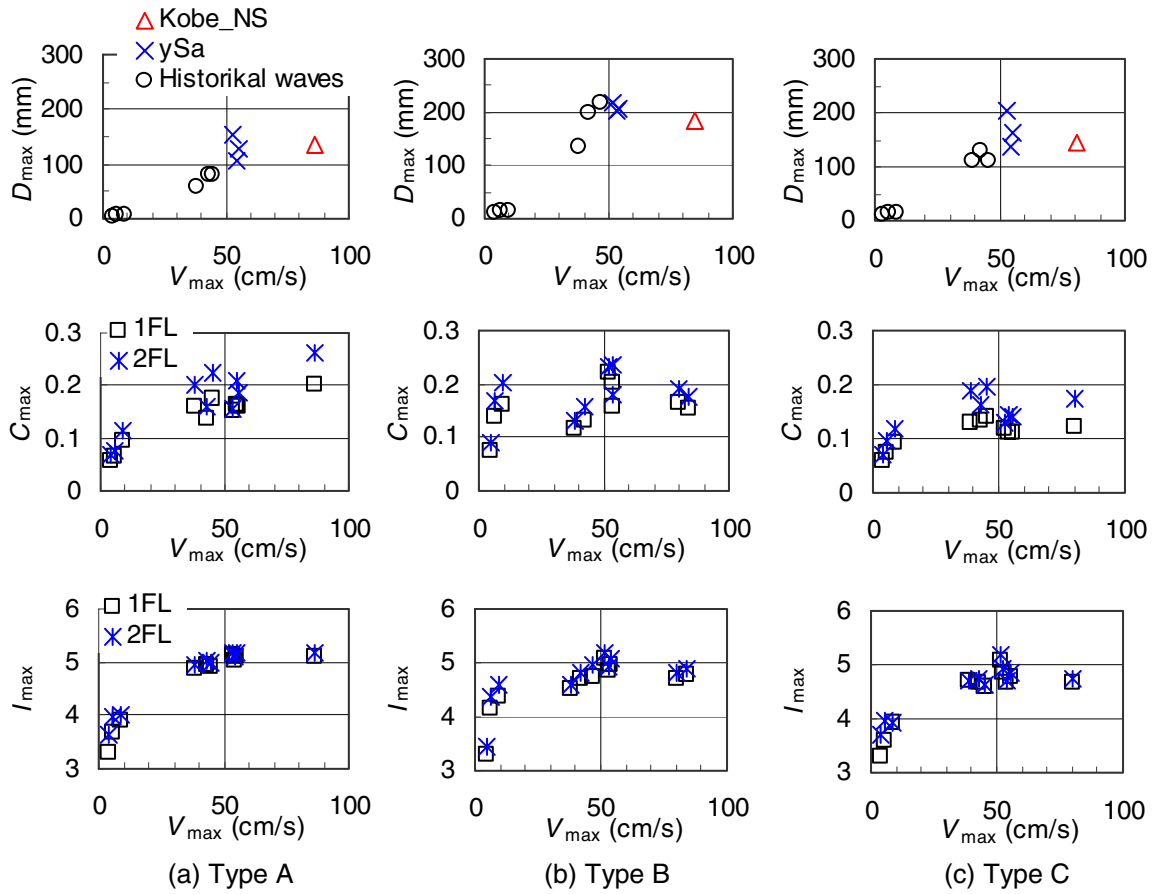
Fig.6. Relationship between input maximum velocity and response maximum value
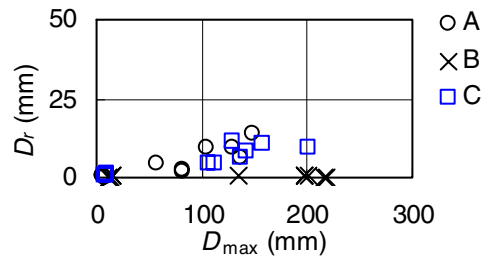(Displacement of the base isolation layer D_{max}, Shear coefficient C_{max}, Seismic intensity I_{max})
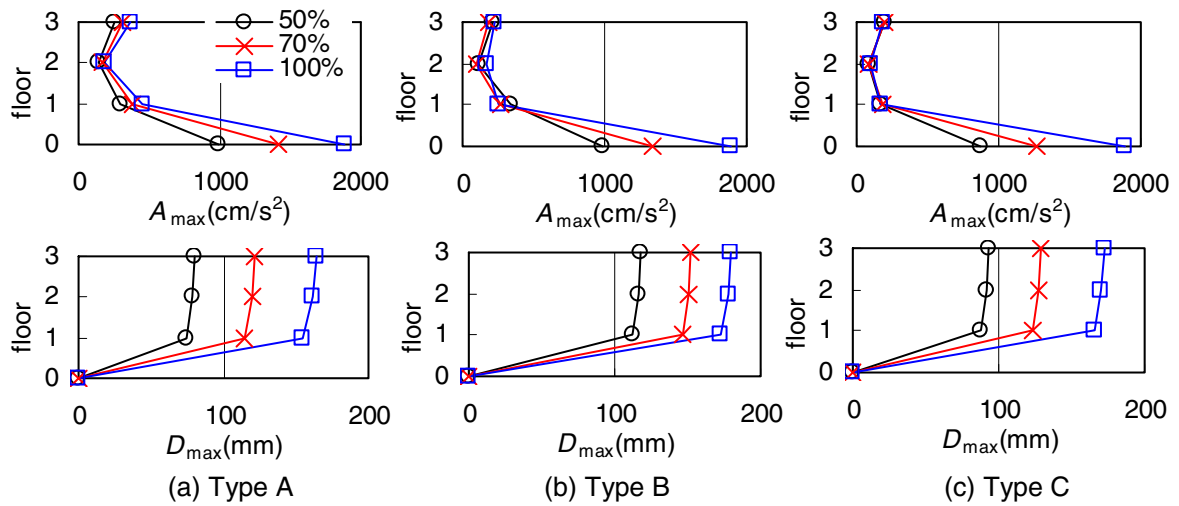
Fig.7. Relationship between input level of the Tarzana wave and response maximum value (Acceleration A_{max}, Displacement D_{max})

Regardless of the type of device, the response acceleration was reduced to 1/3 to 1/6 of the input acceleration. Base isolation layer displacement was within 25 cm, and the story drift angle of the first floor was not greater than 7 mm, indicating that there was no damage. No piece of furniture toppled over, either. Thus, all devices were effective against this type of input wave even against exceptionally high levels of input. The response acceleration of the superstructure did not show significant changes even when input acceleration was doubled. The amounts of change for a Type C device were particularly small: 173 --> 187 cm/ s^2 at the first floor level, 87 --> 97 cm/ s^2 at the second floor level, and 187 --> 192 cm/ s^2 at the roof level. In the case of a Type A device, superstructure displacement somewhat increased as the input level rose. This response is thought to reflect the more or less linear nature of the stiffness of the base isolation layer. The reason why greater response occurred in the case where a Type A device was used than in the cases where other devices were used is thought to be that the capacity of the viscous dampers was slightly too large for the weight of the overlying structure. However, effectiveness of base isolation is obvious even in the case of overdamping like this. As mentioned earlier, reduction of base isolation layer displacement may be thought of as an advantage.

Next, let us discuss residual displacement after ground motion excitation. As the slide initiation load of the base isolation layer is increased so as to achieve a trigger function against wind loads, residual displacement tends to increase. Figure 8 shows the relationship between the maximum displacement D_{max} and residual displacement D_r of the base isolation layer occurring in response to ground motion in single-axis excitation. The point at which the curve representing the nominal restoring force characteristics (Figure 5) takes the value of zero is about 50 mm for a Type A device, 0 mm for a Type B device, and about 140 mm for a Type C device on the horizontal axis. Residual displacement after ground motion response, however, is as small as 13.6 mm or less. It has been reported (Sakamoto et al.[2]) that in the case of a similar slide bearing (μ=0.048) device, differences in the tangential period T_t of the base isolation layer resulted in residual deformations of 2 cm (T_t =3 s) and 7 cm (T_t=4.4 s). In the case of a device with a relatively small coefficient of static friction like the devices used for the purposes of this study, however, if the tangential period is not very long (T_t=3.6 in the test), there will be little need to perform a zero return after encountering a strong earthquake not only in the case of a roller bearing device but also in the case of a slide bearing device.


Fig.8. Maximum displacement D_{max} and residual displacement D_r of the base isolation layer

## Comparison of responses to different input waves

As an example of comparison of response differences due to differences in the dominant period of ground motion, Figure 9 compares response accelerations in the cases of excitation using the Kobe NS wave and the Notification wave $_yS_a100$. The response mode in the excitation using the Kobe wave, which contains a considerable amount of short-period components, is in the shape of the letter "L," while the response mode for the Notification wave $_yS_a$ 100, which is dominated by long-period components, is almost linear. The L-shaped mode occurred because the short-period components of the inputs were not completely removed by the base isolation layer so that the influence of higher modes on the superstructure became noticeable.

This phenomenon occurred not only in the slide bearing device but also in the ball-bearing device (Type A device), which is more prone to load fluctuations during cyclic loading, though the phenomenon in the latter device is less noticeable. It is thought, however, that the amount of response is small enough to be ignored unless the stiffness of the superstructure is extremely low.


(a) Kobe_NS   (b) $_yS_a100$
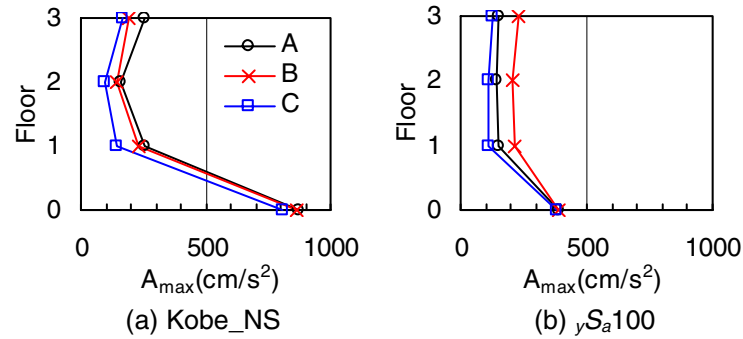
Fig.9. Compares response accelerations to different input waves

Since the input wave of $_yS_a100$ did not attain the target wave on long-period region (Figure 4), it looks at the influence of long-period components in model analysis here. After the response of the input wave set up the analysis model, the response of the target wave was computed. Figure 10 shows the analytical results of the load–deformation relationship for the base isolation layer with different long period components. For devices B and C, large amounts of displacement occurred in connection with the target wave under the influence of long-period components. Cautions are required for devices B and C of the low tangent stiffness to the wave dominated by long-period components.

(a) Type A   (b) Type B   (c) Type C
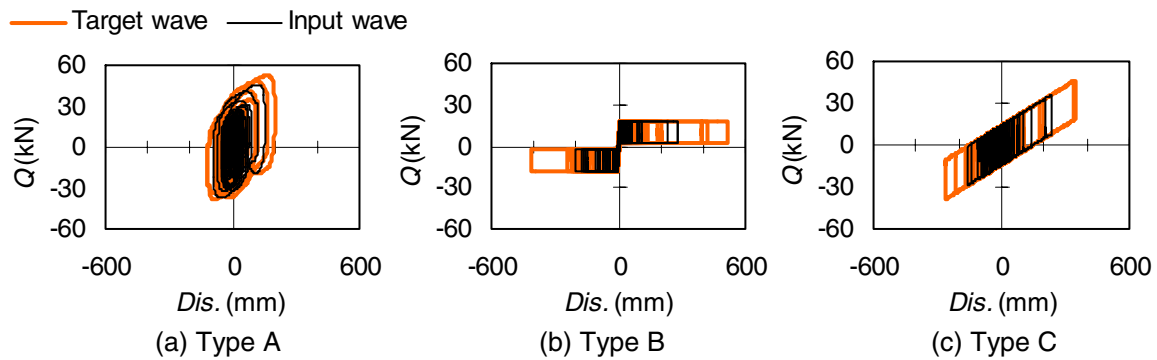
Fig.10. Analytical results in the cases where $_yS_a100$ wave with different long-period components

(a) Kobe wave

(b) Tarzana wave
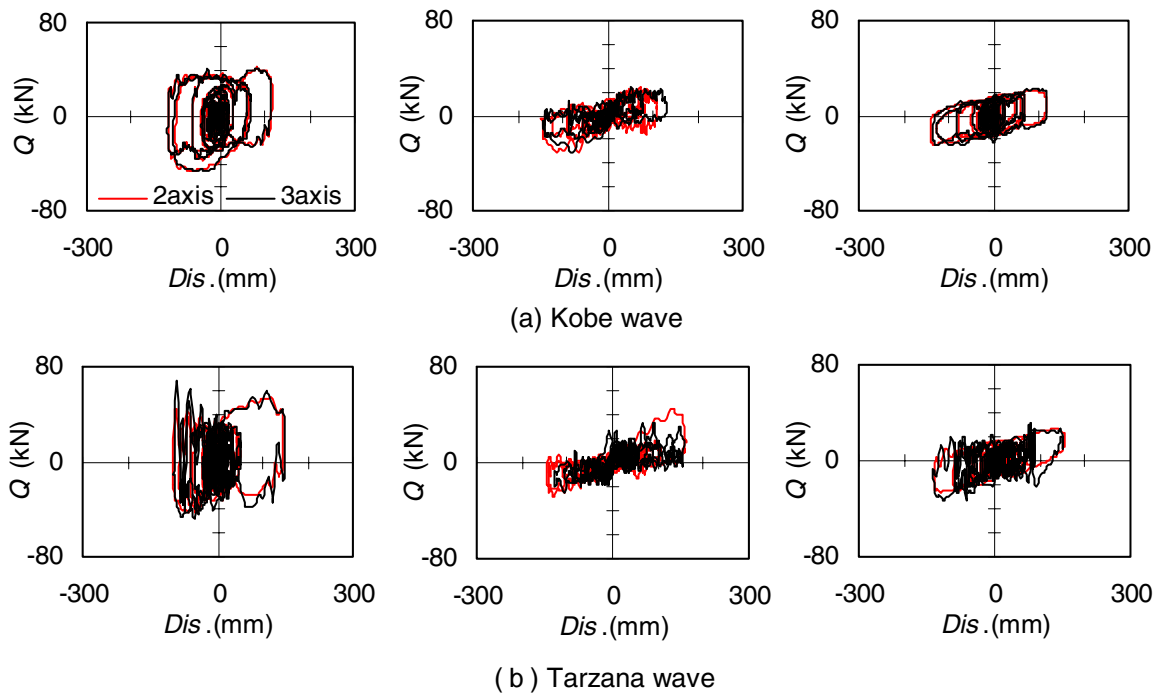
**Fig.11. Influence on the load-deformation relationship for the base
isolation layer by the existence of vertical motion**

Next, let us take a look at the effects of vertical motion input. Figure 11 shows the load–deformation relationship for the base isolation layer in the X direction in the cases of horizontal-two-axis excitation and three-axis excitation (maximum vertical acceleration: 330 cm/s^2 and 1,028 cm/s^2) using the Kobe and Tarzana waves. Compared with the two-axis excitation response, the three-axis excitation response hysteresis loops are characterized by small-scale load fluctuations. Base isolation layer response displacements of the two ball-bearing type devices (A, B) did not show significant differences, but the response displacements of the slide-bearing type device (C) in the three-axis excitation were 6 to 9% smaller. Compared with the two-axis excitation, the response shear coefficient of the superstructure is considerably amplified, particularly with a Type B device subjected to the Kobe wave and with a Type B or Type C device subjected to the Tarzana waves whose vertical motion amplitude exceeds 1G. The maximum story drift angle of the superstructure, however, is only 1/442, which is well within the elastic range.

CONCLUSIONS

The response properties of three types of base isolation devices have been compared under identical conditions and using identical input waves by conducting a shaking table test in which a single house superstructure was used in combination with different types of base isolation devices. All of the devices tested have proved effective so that for the input ground motions used in the test, the response acceleration was sufficiently lower than the input acceleration. No interior or exterior damage was found in the superstructure and bookcases placed in the structure did not topple over. Thus, it has been verified that the tested base isolation devices satisfy the basic performance requirements. The evaluation results are summarized below.

1) Plane ball-bearing type device (Type A device): Since the capacity of the dampers used in the test was too large for the size of the building, the response acceleration of the building superstructure tended to be high. This tendency was particularly noticeable in the response to historical ground motions, but satisfactory results were obtained for long-period ground motions. It is believed that use of small dampers will expand the degrees of freedom in designing base-isolated houses.

2) Ball-in-cone bearing type device (Type B device): Devices of this type proved effective in reducing the response of the superstructure. In cases where the input level is high or the input ground motion contains a high percentage of long-period components, isolation layer displacement may reach the displacement limit of the device. It is therefore necessary either to increase damper capacity or to extend the displacement limit of the device.

3) Plane slide bearing type device (Type C device): The response of the superstructure to each ground motion was effectively reduced. Deformation tended to become large, however, in response to input waves dominated by long-period components. Incorporating viscous damping elements into slide type devices is thought to be a good way to improve the applicability of devices of this type to long-period motions or to reduce deformation.

4) Effects of vertical motion: Effects on upper-level shear were observed in the case of 1G input in the vertical direction, but all base isolation devices proved effective against vertical motions.

5) Residual deformation: As long as a device with a not-so-large coefficient of static friction and a not-so-long tangential period is used as in the test conducted for the purposes of this study, there will be little need to return the device to its original position after encountering a strong earthquake. This applies not only to ball bearings but also to slide bearings.

Base isolation systems designed for houses need to have the ability to stay still under short-return-period wind loads (trigger function) and the ability to resist very rare wind loads by the strength of the isolation layer although this was not verified in the test.

The authors are thinking of conducting follow-up studies on such considerations as how occupants feel when base isolation systems respond to wind loads, maintainability and durability of base isolation devices, and the total cost of base isolation systems. Such studies will facilitate the choice of base isolation devices that make effective use of their characteristics, and will also facilitate the design of base isolation systems, thereby making it possible to present performance options in designing base isolation system.

REFERENCES

1. Iiba,M.,et al.(1999),Three dimensional shaking table test on seismic behavior of isolators for houses Part1-6. In: Summaries of Technical Papers of Annual Meeting of Architectural Institute of Japan; Vol.B-2: 741-752(in Japanese).
2. Sakamoto,I.,et al(1999),An experiment of base-isolated wooden house Part1-9. In: Summaries of Technical Papers of Annual Meeting of Architectural Institute of Japan; Vol.B-2: 715-732(in Japanese).